Surgical and Radiologic Anatomy (2019) 41:1011–1018
https://doi.org/10.1007/s00276-019-02277-w

ORIGINAL ARTICLE

Posterior ethmoid cell expansion towards the inferolateral region of the sphenoid sinus: a computed tomography study

Jinfeng Liu[1] · **Qitong Liu**[2] · **Ningyu Wang**[1]

Received: 6 March 2019 / Accepted: 22 June 2019 / Published online: 27 June 2019

Abstract

Objective The aim of this study was to investigate the anatomical imaging characteristics of posterior ethmoid cells (PEs) expanding towards the inferolateral region of the sphenoid sinus (SS).

Methods This study included a total of 278 inpatients (556 sides) whose paranasal sinus computed tomography (CT) scans were reviewed and collected from May 2018 to February 2019. The anatomical imaging characteristics of PEs expanding towards the inferolateral region of the SS were observed.

Results PEs expanding towards the inferolateral region of the SS formed an inferolateral spheno-ethmoid cell (ISEC). ISECs were observed on three sides (0.54%; 3/556) in three cases (1.08%; 3/278). All of the ISECs were present unilaterally on the right side of the SS. The ISECs originated from the most posterior ethmoid cell; they were first located at the medial aspect of the orbital apex, pneumatized continually backward to the inferomedial wall of the orbital apex, and then extended into the lateral region of the SS. The ISECs further extended laterally, inferiorly and posteriorly beyond the sphenoid body into the greater wing and/or pterygoid process.

Conclusion An ISEC is a rare variation of ethmoid air cells. Preoperative recognition of ISECs is essential to achieve safe and effective endoscopic sinus surgery because of the important anatomical location.

Keywords Ethmoid sinus · Sphenoid sinus · Anatomic variation · Tomography · X-ray · Computed

Abbreviations

EMS	Ethmoid maxillary sinus
ESS	Endoscopic sinus surgery
ICA	Internal carotid artery
ISEC	Inferolateral spheno-ethmoid cell
LRS	Lateral recess of the sphenoid sinus
MS	Maxillary sinus
OA	Orbital apex
PE	Posterior ethmoid cell
RMPE	Retromaxillary posterior ethmoid cell
SS	Sphenoid sinus
SOEC	Supraorbital ethmoid cell

✉ Jinfeng Liu
sanming_1978@163.com

✉ Ningyu Wang
wny@sohu.com

[1] Department of Otorhinolaryngology Head and Neck Surgery, Beijing Chaoyang Hospital, Capital Medical University, Beijing 100020, China

[2] Department of Radiology, Beijing Chaoyang Hospital, Capital Medical University, Beijing 100020, China

Introduction

The ethmoid sinus is not a true nasal sinus in evo-devo theory and is considered part of the skull-base bones [8, 9] unlike the maxillary, frontal and sphenoidal sinuses that result from bone cavitation following red marrow degeneration. Significant anatomical variations without regularity exist in the ethmoid sinus, which is also considerably different from the other three groups of paranasal sinuses [4, 10–13] and is probably due to its evolution.

Currently, expansion of the ethmoid sinus can be divided into the following groups: (1) the anterior group of cells in the frontal sinus ostium, including the agger nasi cell, supra agger cell and supra agger frontal cell; (2) the posterior group of cells in the frontal sinus ostium, including the supra bulla cell, supra bulla frontal cell and supraorbital ethmoid cell (SOEC) [17]; (3) the infraorbital ethmoid cells (IOECs) that surround the maxillary sinus ostium, including the anterior ethmoid cells that extend into the maxillary sinus and are localized in the infraorbital region (Haller's cells) [3] and the posterior ethmoid cells (PEs) that extend towards the maxillary sinus, i.e. the ethmoid maxillary sinus (EMS),

and the retromaxillary posterior ethmoid cells (RMPEs) [7, 11, 12]; and (4) the most posterior ethmoid cell that also pneumatizes superior and lateral to the sphenoid sinus (SS) and forms the Onodi cell [14, 15], which is a significant anatomical variant closely related to the optic nerve. However, no reports on PEs that pneumatize lateral and inferior to the SS are available.

In the present study, we describe a rare anatomical variation of PE pneumatization entering the inferolateral region of the SS and the pterygoid process. We describe this variation as an inferolateral spheno-ethmoid cell (ISEC). The ISECs reported here also provide further evidence of the uncertainty associated with ethmoid variations. Furthermore, ISECs are easily confused with variations of the SS and Onodi cells on computed tomography (CT) because of similar CT characteristics. Therefore, the differences between ISECs and anterior extension of the SS, smaller SSs, lateral recess of the sphenoid sinus (LRS) [16] and Onodi cells based on the drainage channels, location and bony septum of ISECs are detailed in "Discussion".

Study design

We conducted a retrospective analysis of paranasal sinus CT scans obtained from adult inpatients encountered in our hospital from May 2018 to February 2019. CT was performed in the Radiological Department, Beijing Chaoyang Hospital, Capital Medical University. We included a total of 278 patients (556 sides) whose paranasal sinus CT scans were reviewed and analysed.

The enrolment criteria were as follows: (1) no history of head or sinus injury; (2) no history of sinonasal surgery; (3) clear PE and SS anatomical structures; and (4) age older than 18 years. The exclusion criteria were as follows: (1) a history of sinus surgery or sinus trauma; (2) CT findings of sinonasal disease (e.g. neoplasm, fungal sinusitis, osteofibroma, fibrous dysplasia or chronic rhinosinusitis) involving the PEs or SS; and (3) CT findings of a craniofacial abnormality (e.g. craniofacial cleft, orbital hypertelorism, or craniostenosis) [11].

CT examination and analysis

The CT scanning range spanned from the superior margin of the frontal sinuses to the inferior margin of the maxillary alveolar process. A GE Lightspeed 64-slice spiral CT (USA) system was used with a bone imaging algorithm. CT scans were obtained at a section thickness of 0.625 mm, an interval of 0.5 mm. The following parameters of acquisition were employed: kV: 120, mAs: 320, collimation: 40 × 0.6 mm, tube rotation: 1 s, matrix size: 512 × 512; reconstruction thickness: 3 mm.

The GE system was used to obtain multiplanar reconstructions (MPRs) in the three anatomical planes. GE Centricity Enterprise Web 3 software (GE Medical Systems) was used for viewing and measuring. Continuous observation was performed by sliding the computer mouse. Collection of the CT scans was approved by the Ethics Committee of Capital Medical University affiliated with Beijing Chaoyang Hospital. The study also adhered to the guidelines of the Declaration of Helsinki.

Determination of ISECs

The diagnosis of an ISEC was determined when PE pneumatization entering the inferolateral region of the SS (the greater wing or the pterygoid process of the SS), which drains directly into the most posterior ethmoid cell, was observed on the lateral side of the superior turbinate (Figs. 1, 2, 3, 4, 5 and 6). ISEC identification was performed by one otolaryngologist (LJ), and ISECs were confirmed by two otolaryngologists together (LJ and WN).

Determination of Onodi cells

The Onodi cell is the most posterior ethmoidal air cell that pneumatizes superolateral, superior or lateral to the SS, and surrounds the optic channel (Figs. 2, 4 and 6) [14].

Determination of the LRS

The line connecting the medial edge of the anterior opening of the vidian canal (V) and the extracranial end of the foramen rotundum (the VR line) is the demarcation between the sphenoid body and lateral parts of the sphenoid bone. The LRS is defined as the lateral cavity of the SS extending from the main sphenoid cavity beyond the VR line into the greater wing and/or pterygoid process (Figs. 2 and 4) [16].

Determination of the anterior recess of the SS

An anterior recess of the SS originating from the lateral portion of the anterior wall of the SS was identified when the recess extended anteriorly beyond a horizontal line along the sinus side of the sphenoid crest on axial CT (Fig. 7) [16].

Statistical analysis

Data regarding patient age are presented in the form of the mean ± standard deviation (SD). The descriptive statistics were determined using SPSS (version 16.0, SPSS, Inc., USA). The incidence rates of ISECs were calculated with preservation of two decimal places.

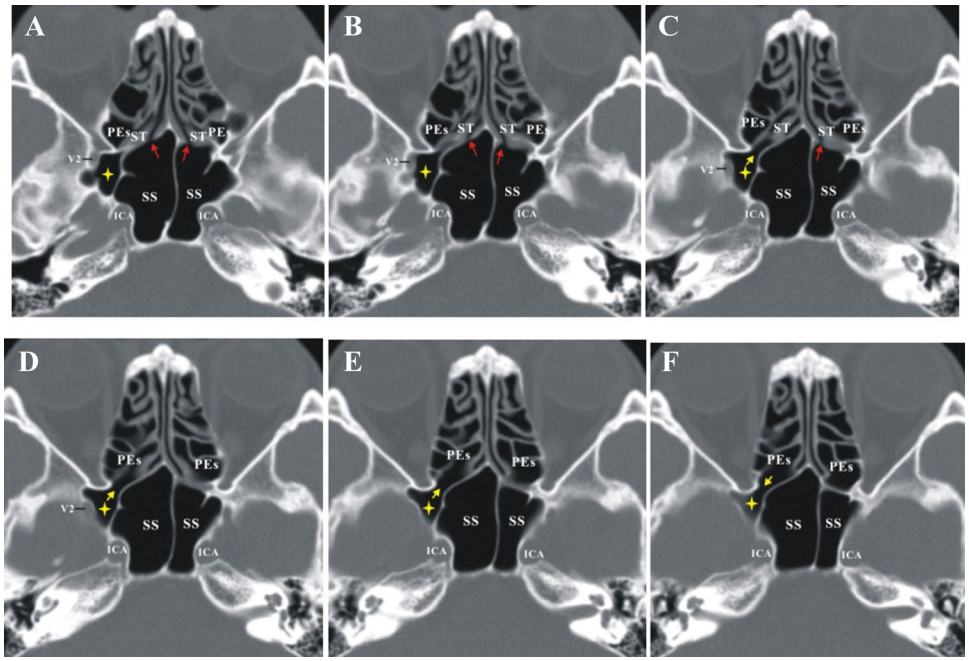

Fig. 1 An axial CT scan of the bottom-up series showing the ISEC (indicated by yellow asterisks) in case 1. The ISEC is the result of the pneumatization of the greater wing of the sphenoid bone and the pterygoid process, which is separated from the main cavity of the SS by bone. **a**, **b** Both sides of the SS have independent drainage channels (indicated by red arrows) to the sphenoethmoidal recess. **c**–**f** The ISEC drains into the PEs. The drainage channel of the ISEC is located on the lateral side of the superior turbinate (indicated by yellow arrows) (colour figure online)

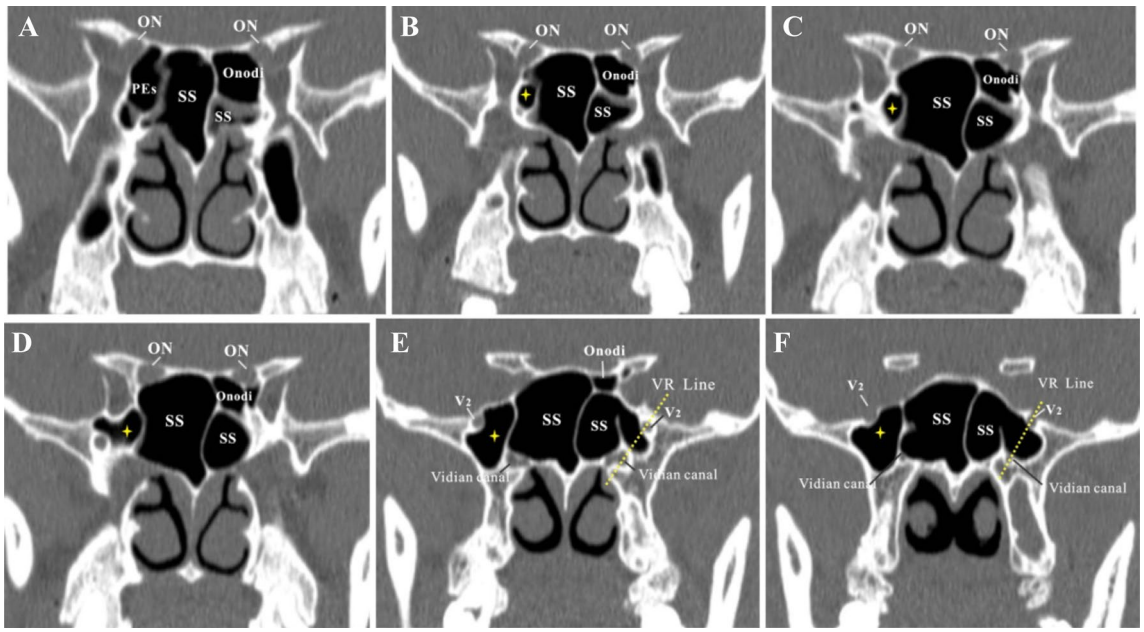

Fig. 2 A series of coronal CT scans showing that the PEs expand into the SS to form an ISEC (**a**–**f**) posteriorly and laterally in case 1. The yellow asterisks in **b** and **c** indicate the ostium of the ISEC. The yellow asterisks in **d**–**f** indicate the ISEC. The ISEC extends towards the inferolateral region of the SS and away from the optic canal and is significantly lower than the Onodi cell (**b**–**e**). The Onodi cell is close to the optic canal. The ISEC is close to the orbital apex, maxillary nerve and cavernous sinus (**d**–**f**). The left SS extends laterally and forms the LRS, which is connected with the main cavity of the SS (**e**, **f**) (colour figure online)

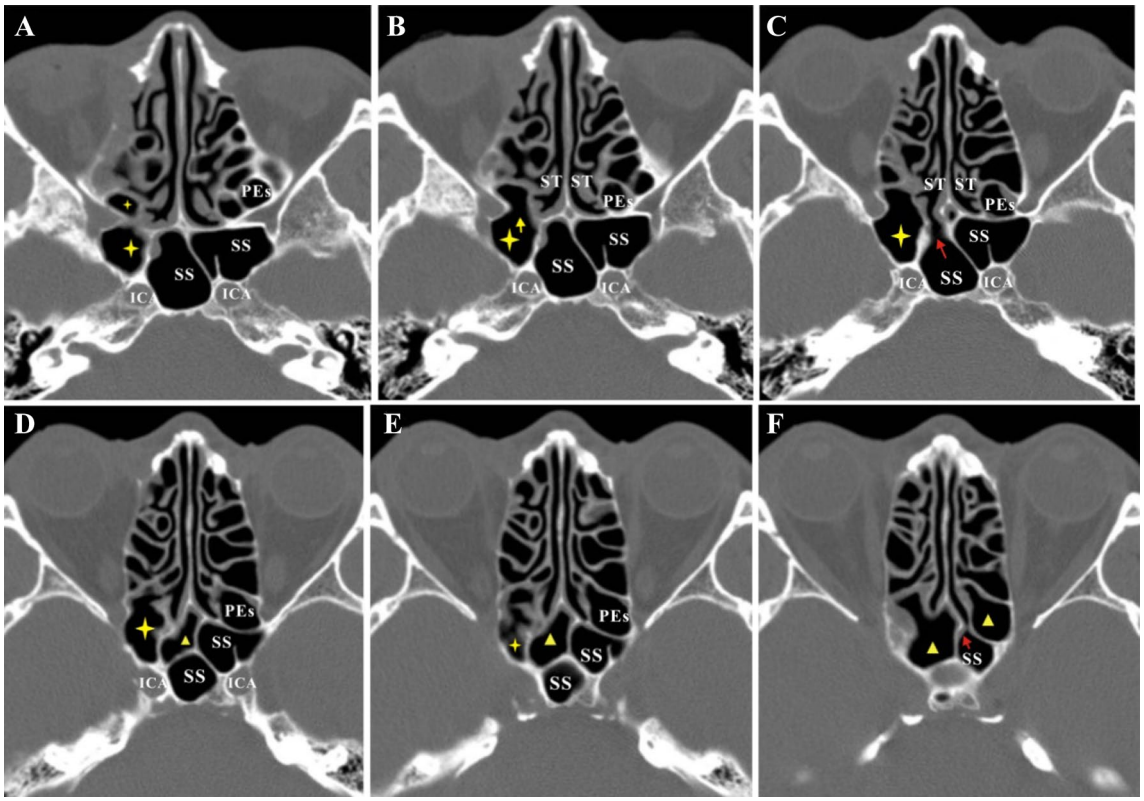

Fig. 3 **a**–**f** Axial CT scans of the bottom-up series showing the ISEC (indicated by yellow asterisks) in case 2. The Onodi cell (indicated by solid yellow triangles in **d**–**f**) is located superomedial to the ISEC. The ISEC looks similar to a dumbbell and drains into the PEs (indicated by yellow arrows) (**b**). The drainage channels of the SS (indicated by red arrows) connected to the sphenoethmoidal recess (**f**). **a**–**d** The posterior end of the septum between the ISEC and the SS is attached to the protrusion of the ICA. The posterior part of the ISEC is adjacent to the ICA (colour figure online)

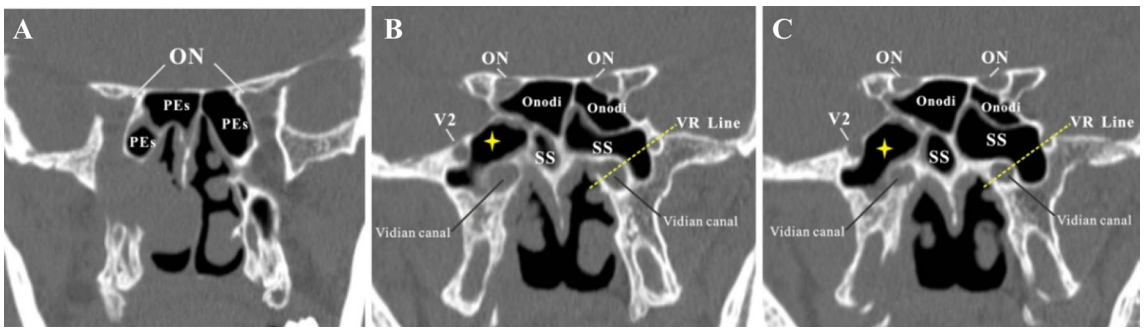

Fig. 4 A series of coronal CT scans distinguishing the ISEC from the Onodi cell and LRS in case 2. **a** The PEs extend towards the SS. **b**, **c** The PEs extend towards the superolateral region of the SS; the Onodi cell is present on both sides of the SS and surrounds the optic channel. At the same time, the right PEs expand towards the inferolateral region of the SS, where the ISEC is present (indicated by yellow asterisks). All of the Onodi cell is above the ISEC. The left SS extends laterally and forms the LRS, which is connected with the main cavity of the SS (colour figure online)

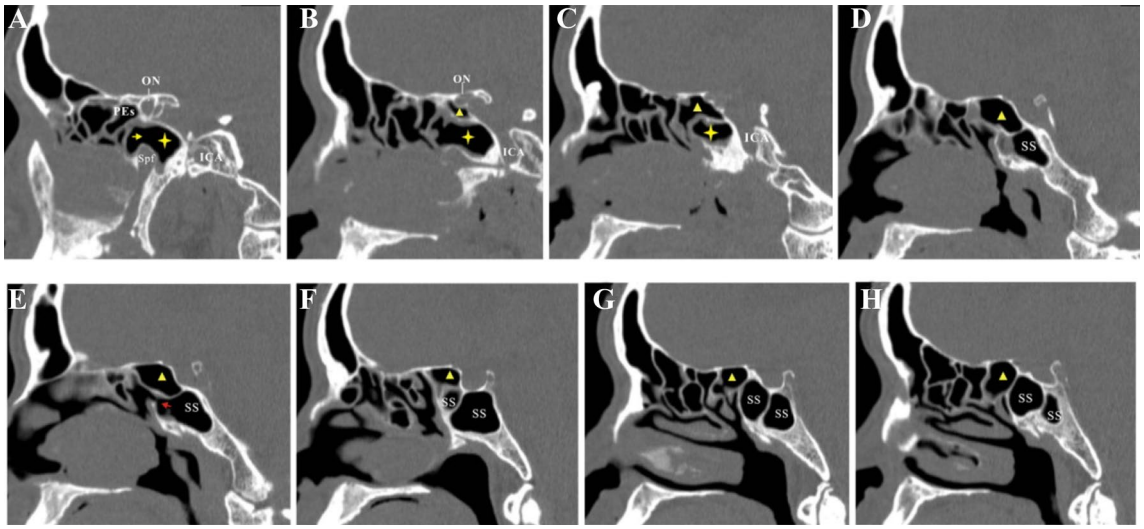

Fig. 5 A series of sagittal CT scans from right to left showing differences between the ISEC and Onodi cell in case 2. **a** The ISEC (indicated by yellow asterisks) is shaped similar to a dumbbell and passes above the sphenopalatine foramen. **b–d** The posterior region of the ISEC is adjacent to the ICA. The Onodi cell (indicated by solid yellow triangles) is located above the ISEC and SS. **a–h** The gradual change in the bilateral Onodi cells and SSs from right to left. The drainage channels of the right SS are indicated by the red arrow in **f** (colour figure online)

Fig. 6 The relationships among the ISEC, Onodi cell and SS in case 3. **a–c** Axial CT scans of the bottom-up series showing the ISEC (indicated by yellow asterisks) and the SS. The drainage channels of the right SS are indicated by the red arrow in **c**. **d–f** A series of coronal CT scans from front to back showing isolated inflammation in the Onodi cell. The pneumatization of the right PEs expands towards the SS and forms both the ISEC and the Onodi cell. The Onodi cell is located superomedial to the ISEC and superolateral to the SS (colour figure online)

Results

ISEC morphology and anatomy

The paranasal sinus CT images of 278 patients (556 sides) ranging in age from 18 to 73 years (mean, 42.32 ± 13.70 years) were reviewed and analysed. Based on the present observations, PE pneumatization entering the inferolateral region of the SS is a rare variant that only appeared on three sides (0.54%; 3/556) in three cases (1.08%; 3/278). Case 1 is a 33-year-old male patient with nasal obstruction and posterior nasal drip (Figs. 1 and 2). Case 2 is a 56-year-old male patient with adenoid cystic carcinoma of the maxillary sinus (Figs. 3, 4 and 5). Case 3 is a 38-year-old female patient with chronic rhinosinusitis (CRS) (Fig. 6). All ISECs were unilateral and present on the right side of the SS (Figs. 1, 2, 3, 4, 5, 6 and 7).

The ISECs originated from the most posterior ethmoid cells and were first located at the medial level of the orbital

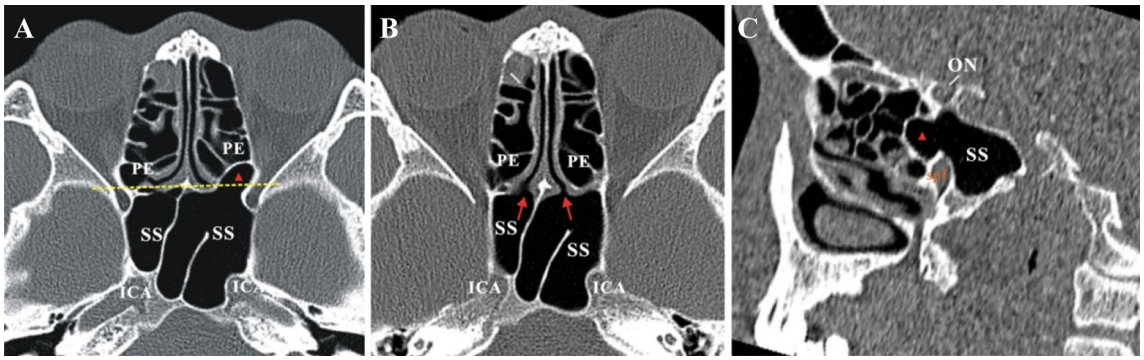

Fig. 7 Anterior extension of the SS. **a** The left SS extending anteriorly and laterally beyond the sphenoid crest. The drainage channels of the SS are indicated by the red arrows in **b**. The anterior recess of the SS is indicated by a solid red triangle in **a** and **c**. The sagittal CT scan in **c** shows that the anterior extension of the SS is shaped similar to a dumbbell and passes above the sphenopalatine foramen (spf) (colour figure online)

apex (Fig. 2b, c). Then the pneumatization continued backward to the inferomedial wall of the orbital apex, extended into the lateral region of the SS, and further extended laterally, inferiorly and posteriorly beyond the sphenoid body into the greater wing and/or pterygoid process (Figs. 1, 2, 3, 4, 5 and 6).

In general, the ISECs can be divided into two parts, including one part in the sphenoid bone and another in the PE. The point where the ISEC pneumatizes into the SS is narrower because the lateral and inferior parts of the ISEC at this site are restricted by the orbital apex and sphenopalatine foramen, respectively, which also causes the ISEC to assume a shape similar to that of a dumbbell on axial and sagittal CT (Figs. 1 and 5). To facilitate correspondence with the SS ostium, the narrower point of the ISEC is described as the ISEC ostium, which is located superior to the sphenopalatine foramen (Figs. 2b and 5a).

Structures adjacent to the ISEC

The structures adjacent to the ISEC in the PE were mainly the orbit, orbital apex, and sphenoid bone, similar to the LRS. In the sphenoid bone part of the ISEC, the anterosuperior wall was adjacent to the superior orbital fissure and passed through the structure (Figs. 2 and 4), and the posterosuperior wall was adjacent to the maxillary nerve and cavernous sinus (Figs. 2d–f and 4b, c). The maxillary nerve was often protruding into this part of the ISEC (2/3 cases) (Figs. 2e and 4b). The medial side of the ISEC was safe, adjacent only to the main cavity of the SS and completely separated from the SS by the osseous septum. This osseous septum was attached to the front of the internal carotid artery (ICA) protrusion and could be adjacent to the ICA (1/3 cases) (Fig. 3). The posterior boundary of the ISEC could reach the anterior part of the foramina ovale and the carotid canal (Figs. 3 and 5). The bottom of the ISEC was the root of the pterygoid and its subsidiary structures.

Discussion

PE pneumatization extending to the inferolateral region of the SS and into the great wing of the sphenoid bone and the pterygoid process is a rare variant and only appeared on three sides (0.54%; 3/556) in three cases (1.08%; 3/278) in the present study. We describe this variation as an inferolateral spheno-ethmoid cell (ISEC). Additionally, no related reports of this variant are available in the literature. PE pneumatization expanded upward and around across the pterygopalatine fossa, into the anterior region of the SS, and further into the greater wing of the sphenoid bone and the pterygoid process laterally and inferiorly (Figs. 1 and 4).

ISECs are not the accessory sphnoid sinus, but are originate from the PEs and expand to the inferolateral region of the sphenoid sinus, based on the theory of paranasal sinus evolution, embryonic development and the morphological characteristics of ISECs. From an embryological point of view and the evo-devo concept of paranasal sinus development, the ethmoid is different from all the other sinuses [8, 9]. The ethmoid bone originates from the cartilaginous nasal capsule or paleosinus (endochondral bone), whereas the other paranasal sinuses are extensions from the ethmoid into membranous bone via epithelial diverticula extensions [13]. The endochondral bony origin of the ethmoid sinuses leads to remarkably thin bony contours with irregular and morphologically unique borders, making them substantially different from the other paranasal sinuses [13]. Compared with ISECs (Figs. 1, 2, 3 and 5) and the anterior extension of the SS (Fig. 7), the medial wall and anterior structure of the ISEC appeared as thin bony contours, while the anterior structure of anterior

extension of the SS was thicker. This finding is consistent with the origin of ISECs from the ethmoid sinus. Furthermore, the ethmoid sinus is easy to pneumatize beyond where it should be and extends to other sinuses, affecting the drainage of other sinuses [13]. Based on the characteristics of pneumatization and development of the ethmoid sinus, similar to other extended types of ethmoid sinuses (agger cells, Haller's cells, SOEC, EMS, RMPEs and Onodi cells) widely reported in the literature [3, 7, 10–15, 17], we also think that ISECs originate from the ethmoid sinus. Finally, the drainage channel of the ISECs also supports the origin of the ISECs from PEs, rather than the accessory sphenoid sinus. The SS ostium has been considered one of the most constant and reliable landmarks. It always appears in the anterior wall of the SS and drains into the sphenoethmoidal recess [6] and is always located at the media side of the superior turbinate [5]. In contrast, in the present study, the ISEC drainage channel opens into PEs on the lateral side of the superior turbinate, which is not in line with the drainage characteristics of the sphenoid sinus. However, similar to our cognitive dilemma about Haller's cell [3], we cannot completely rule out the possibility of an inaccurate understanding of the origin of the ISEC.

PEs can extend towards the infraorbital region along the LP and localize between the orbital floor and the maxillary sinus (MS). PEs extend towards the infraorbital region and enter the MS through the maxillary hiatus of the ethmomaxillary sinus (EMS), and RMPEs spread from outside the MS [7, 11, 12]. Both ISECs and RMPEs are PEs located behind the MS. However, RMPEs were located under the orbit without expanding into the sphenoid bone unlike the ISECs in this study. The variations in PEs expanding towards the inferolateral wall of the SS observed in this work are also different from the Onodi cell. Both types of cells are formed by PEs expanding backward to the SS, but a significant difference exists between the two cells. The Onodi cell is formed from pneumatized PEs located lateral and superior to the SS [14, 15]. However, an ISEC is formed from PEs expanding inferolateral to the SS, including pneumatization of the greater wing of the sphenoid bone and the pterygoid process, which is below the orbital apex and optic canal, and then distally away from the optic canal when it extends into the SS. The Onodi cell is often encountered in clinical practice and was present in 50.8% of the sides studied by Wada et al. [15]. The optic nerve is often exposed to Onodi cells [14, 15]. In contrast, an ISEC is similar to an LRS in that the pterygoid and maxillary nerves may be exposed to the ISEC. In addition, Onodi cells appeared in all three cases of ISEC, suggesting excessive PE pneumatization. However, distinguishing an ISEC from an Onodi cell is easier when the ISEC and Onodi cell appear on the same side (2/3 cases). The Onodi cells were located superomedial to the ISECs in this study (Figs. 4, 5 and 6).

Many variations exist in the pneumatization of the SS [1, 2, 6], which is easily confused an ISEC on CT. In particular, LRSs (Figs. 2 and 4), anterior extensions of the SS (Fig. 7) and smaller SSs show characteristics on CT similar to those of ISECs. However, these entities can be distinguished based on the drainage channels, location and relationship with the SS cavity. First, obvious differences exist between an ISEC and LRS. An ISEC is completely separated from the main cavity of the SS by a thicker bone plate. The ISEC drainage channel opens in PEs on the lateral side of the superior turbinate [5]. In contrast, an LRS is only a lateral expansion of the SS cavity that opens into the sphenoethmoidal recess. Second, in some patients, both sides of the SS develop extremely asymmetrically, with one side fully pneumatized and almost filling the whole sphenoid body and the other side only as large as a pea and may be easily confused with an ISEC. However, a clear difference exists between the drainage channels of the two groups of cells. The SS ostium has been considered one of the most constant and reliable landmarks for endoscopic sinus surgery (ESS) [1, 2, 6]. It always appears in the anterior wall of the SS and drains into the sphenoethmoidal recess, even in smaller SSs. Based on the present observations, the ISECs drained directly into the most posterior ethmoid cell, which was obviously different from the drainage of smaller SSs. Finally, anterior extension of the SS also has a similar dumbbell shape and runs through the ethmoid and sphenoid regions superiorly across the sphenopalatine foramen, which is similar to the ISECs on coronal and sagittal CT (Fig. 7). However, anterior extension of the SS is only pneumatization of the SS extending forward and beyond the normal anatomical scope of the SS anterior wall. The normal SS ostium still drains directly into the sphenoethmoidal recess (Fig. 7), which is different from ISEC drainage. Moreover, in the patients with an ISEC, the SS was located medial to the ISEC (Figs. 1, 2, 3, 4 and 5).

ISECs may be similar to other anatomical variations in the sinus and are not associated with sinusitis, but they still must be considered in ESS. Important structures near the ethmoid sinus are usually in danger during surgery due to extreme variability [10, 14, 15]. ISECs must also be identified before ESS because of their important anatomical location. The adjacent structures superior and lateral to ISECs include the orbital apex, maxillary nerve, and cavernous sinus. Moreover, the roof of the ISEC is lower than the roof of the SS. The roof of the SS is used as the upper boundary of the ethmoid sinus when applying the Wigand strategy from back to front in ESS. If the ISEC cannot be accurately identified before the operation, the structures passing through the orbital apex may be injured.

PE inflammation may involve the ISEC because of pneumatization of the ISEC from the PEs. In the treatment of

CRS involving PEs, the ISEC ostium should also be enlarged during ESS to facilitate the clearance of lesions within. However, based on the present observations, although the ISEC ostium may be larger than the SS ostium, opening and expansion of the ISEC ostium during ESS is also difficult and risky. The ISEC ostium should not be extended outward, upward or downward because of the important adjacent structures. The medial side of the ISEC is safe as a thicker osseous septum separates it from the SS. Therefore, to expand the ISEC ostium inward, this osseous septum may need to be removed after resection of PEs to establish a common drainage channel with the SS. In addition, similar to the accessory septum of the SS, this osseous septum likely emerges from the channel of the ICA (Fig. 3). Therefore, we must be aware of the presence of the ICA behind the ISEC and avoid injuring it while removing the osseous septum during ESS.

Conclusions

ISECs are formed from PEs that pneumatize and enter the inferolateral side of the SS. This variation of PEs provides further evidence for the uncertainty associated with ethmoid variations. At the same time, preoperative recognition of ISECs is essential to achieve safe and effective ESS.

Acknowledgements The general work was supported by the Beijing Natural Science Foundation (7162066) and the National Natural Science Foundation of China (no. 81271090/H1304).

Author contributions JL discovered and identified this anatomical variation, analysed the clinical significance of this variation, and wrote the manuscript. NW and JL reconfirmed this anatomical variation together. QL completed the image editing.

Compliance with ethical standards

Conflict of interest The authors have no relevant competing interests to declare in relation to this manuscript.

References

1. Anusha B, Baharudin A, Philip R, Harvinder S, Shaffie BM (2014) Anatomical variations of the sphenoid sinus and its adjacent structures: a review of existing literature. Surg Radiol Anat 36(5):419–427. https://doi.org/10.1007/s00276-013-1214-1
2. Anusha B, Baharudin A, Philip R, Harvinder S, Shaffie BM, Ramiza RR (2015) Anatomical variants of surgically important landmarks in the sphenoid sinus: a radiologic study in Southeast Asian patients. Surg Radiol Anat 37(10):1183–1190. https://doi.org/10.1007/s00276-015-1494-8
3. Caversaccio M, Boschung U, Mudry A (2011) Historical review of Haller's cells. Ann Anat 193(3):185–190. https://doi.org/10.1016/j.aanat.2011.02.006
4. Gibelli D, Cellina M, Gibelli S, Cappella A, Oliva AG, Termine G, Sforza C (2018) Anatomical variants of ethmoid bone on multidetector CT. Surg Radiol Anat 40(11):1301–1311. https://doi.org/10.1007/s00276-018-2057-6
5. Gotlib T, Kuźmińska M, Sokołowski J, Dziedzic T, Niemczyk K (2018) The supreme turbinate and the drainage of the posterior ethmoids: a computed tomographic study. Folia Morphol (Warsz) 77(1):110–115. https://doi.org/10.5603/FM.a2017.0067
6. Gupta T, Aggarwal A, Sahni D (2013) Anatomical landmarks for locating the sphenoid ostium during endoscopic endonasal approach: a cadaveric study. Surg Radiol Anat 35(2):137–142. https://doi.org/10.1007/s00276-012-1018-8
7. Herzallah IR, Saati FA, Marglani OA, Simsim RF (2016) Retromaxillary pneumatization of posterior ethmoid air cells: novel description and surgical implications. Otolaryngol Head Neck Surg 155:340–346. https://doi.org/10.1177/0194599816639943
8. Jankowski R, Rumeau C, de Saint Hilaire T, Tonnelet R, Nguyen DT, Gallet P, Perez M (2016) The olfactory fascia: an evo-devo concept of the fibrocartilaginous nose. Surg Radiol Anat 38(10):1161–1168. https://doi.org/10.1007/s00276-016-1677-y
9. Jankowski R, Nguyen DT, Poussel M, Chenuel B, Gallet P, Rumeau C (2016) Sinusology. Eur Ann Otorhinolaryngol Head Neck Dis 133(4):263–268. https://doi.org/10.1016/j.anorl.2016.05.011
10. Jinfeng L, Jinsheng D, Xiaohui W, Yanjun W, Ningyu W (2017) The pneumatization and adjacent structure of the posterior superior maxillary sinus and its effect on nasal cavity morphology. Med Sci Monit 23:4166–4174. https://doi.org/10.12659/msm.903173
11. Liu J, Dai J, Wen X, Wang Y, Zhang Y, Wang N (2018) Imaging and anatomical features of ethmomaxillary sinus and its differentiation from surrounding air cells. Surg Radiol Anat 40(2):207–215. https://doi.org/10.1007/s00276-018-1974-8
12. Liu JF, Liu QT, Liu JY, Yan ZF, Wang NY (2018) CT observation of retromaxillary posterior ethmoid. Lin Chung Er Bi Yan Hou Tou Jing Wai Ke Za Zhi 32(2):121–124. https://doi.org/10.13201/j.issn.1001-1781.2018.02.011 **(Chinese)**
13. Márquez S, Tessema B, Clement PA, Schaefer SD (2008) Development of the ethmoid sinus and extramural migration: the anatomical basis of this paranasal sinus. Anat Rec (Hoboken) 291:1535–1553. https://doi.org/10.1002/ar.20775
14. Özdemir A, Bayar Muluk N, Asal N, Şahan MH, Inal M (2019) Is there a relationship between Onodi cell and optic canal? Eur Arch Otorhinolaryngol 276(4):1057–1064. https://doi.org/10.1007/s00405-019-05284-0
15. Wada K, Moriyama H, Edamatsu H, Hama T, Arai C, Kojima H, Otori N, Yanagi K (2015) Identification of Onodi cell and new classification of sphenoid sinus for endoscopic sinus surgery. Int Forum Allergy Rhinol 5(11):1068–1076. https://doi.org/10.1002/alr.21567
16. Wang J, Bidari S, Inoue K, Yang H, Rhoton A Jr (2010) Extensions of the sphenoid sinus: a new classification. Neurosurgery 66(4):797–816. https://doi.org/10.1227/01.NEU.0000367619.24800.B1
17. Wormald PJ, Hoseman W, Callejas C, Weber RK, Kennedy DW, Citardi MJ, Senior BA, Smith TL, Hwang PH, Orlandi RR, Kaschke O, Siow JK, Szczygielski K, Goessler U, Khan M, Bernal-Sprekelsen M, Kuehnel T, Psaltis A (2016) The international frontal sinus anatomy classification (IFAC) and classification of the extent of endoscopic frontal sinus surgery (EFSS). Int Forum Allergy Rhinol 6(7):677–696. https://doi.org/10.1002/alr.21738